Electron localisation in nonstoichiometric films of aluminium nitride produced by reactive sputtering

1987 J. Phys. C: Solid State Phys. 20 565

(http://iopscience.iop.org/0022-3719/20/4/008)

J. Phys. C: Solid State Phys. **20** (1987) 565–583. Printed in the UK

Electron localisation in non-stoichiometric films of aluminium nitride produced by reactive sputtering

N Fortier and R R Parsons
Department of Physics, University of British Columbia, Vancouver, British Columbia, Canada, V6T 2A6

Received 3 March 1986

Abstract. Thin films of non-stoichiometric aluminium nitride of various compositions (AlN_x, with $0 \leqslant x \leqslant 1$) were fabricated using planar magnetron sputtering. Three different transport regimes have been observed. The transport properties of films with room temperature conductivity above $10^4\ \Omega^{-1}\ cm^{-1}$ are found to be well described by the semi-classical Boltzmann equations. In films with room temperature conductivity between $10^4\ \Omega^{-1}\ cm^{-1}$ and $100\ \Omega^{-1}\ cm^{-1}$ the conductivity is found to be dominated by electron localisation effects while the thermoelectric power remains free-electron like. This is seen as indicating that the density of states remains unaffected as localisation effects set in. The temperature dependence of films with room temperature conductivity between $0.5\ \Omega^{-1}\ cm^{-1}$ and $10^{-3}\ \Omega^{-1}\ cm^{-1}$ is found to be well described by the equation $\sigma(T) = \sigma_0 T^{-p} \exp(T_0/T)^{-s}$, with $s = \frac{1}{4}$, thus suggesting that the conduction proceeds by variable-range hopping. Limits on the value of p are established and are used to show that only one theory of variable-range-hopping is consistent with such a temperature dependence.

1. Introduction

A considerable amount of work has been devoted recently, both experimentally [1–15] and theoretically [16–29], to the study of transport properties in disordered materials. In materials exhibiting little disorder, the traditional approach has been to assume that the scattering of the conducting electrons by a random potential (e.g. impurities) causes the electron wavefunctions (Bloch waves) to lose phase coherence on the length scale of their mean free path. Nevertheless, the wavefunctions remain extended. The electronic motion has a ballistic character, the interaction of the conducting electrons with electric field, temperature gradient etc, being described by classical equations of motion (Boltzmann approach). On the other hand, in strongly disordered materials, Anderson [30] has pointed out that the wavefunctions can become localised, with their envelopes decaying exponentially from their localisation points in space. The conduction in these materials is expected to proceed via nearest-neighbour hopping and/or variable-range hopping.

More recently, Abrahams *et al* [31] have proposed a scaling theory of the conductivity, which encompasses the limits of weak and strong disorder but also reveals the existence of an intermediate regime of moderate disorder leading to an unexpected correction

0022-3719/87/040565 + 19 $02.50

to the Boltzmann conductivity (σ_b). For three-dimensional systems at $T = 0\,K$ this correction to the conductivity (σ) is given by [19]

$$\sigma(0)/\sigma_b(0) = 1 - [3/(K_f l_e)^2](1 - l_e/L) \tag{1}$$

where l_e is the elastic mean free path, L a length scale related to the size of the sample, and K_f the Fermi wave-vector. At finite temperature L must be replaced by the inelastic diffusion length $L_i = ((l_e l_i)/3)^{1/2}$, where l_i is the inelastic mean free path [2].

Arguing that the electronic motion in moderately disordered materials is diffusive, Kaveh and Mott [17, 18] have reproduced the scaling result of Abraham *et al* [31] using diffusion equations. They have also shown [19] that the correction to the Boltzmann conductivity can be obtained using wavefunctions of the form Ψ_{ext}/r^2, where Ψ_{ext} is an extended wavefunction, and calculating the conductivity using the Kubo–Greenwood formalism [20].

Three qualitatively different transport regimes seem to emerge from these theoretical treatments, each one characterised by a different wavefunction. In the weak disorder limit the wavefunctions are extended and the transport properties well described by the semi-classical Boltzmann equation. In the moderate disorder limit the wavefunctions are considered to be 'power-law' localised and therefore the conductivity is characterised by a universal temperature dependence, as described by Kaveh and Mott [21]. In the limit of strong disorder, the wavefunctions are expected to be exponentialy localised and therefore the conductivity is determined by nearest-neighbour hopping and/or variable-range hopping.

The transport properties of non-stoichiometric films of aluminium nitride produced by planar magnetron sputtering [32] have been examined. The three transport regimes described above have been observed. The objective of the paper is threefold. First, it is shown that the DC conductivity of samples characterised by moderate disorder is accurately described by Kaveh and Mott equation [2, 21]:

$$\sigma(T) = \sigma_b(0)\left(1 - \frac{3}{(K_f l_e)^2}\right) + \sigma_b(0)\left(\frac{3}{(K_f l_e)^2}\frac{l_e}{L_i} - \frac{l_e}{l_i}\right). \tag{2}$$

Estimates of l_e and l_i as well as of K_f are given and are used to demonstrate that equation (2) provides an accurate description of the temperature dependence and magnitude of the conductivity of these films. Second, it is shown that in this regime the thermoelectric power exhibits a free-electron behaviour, suggesting that the density of states $N(E)$ does not significantly change as localisation effects set in. Third, in the strong disorder limit, it is shown that the temperature dependence of the conductivity is well described by $\sigma(T) = \sigma_0 T^{-p} \exp(T_0/T)^{-s}$ with $s = \frac{1}{4}$, thus indicating that the conductivity proceeds by variable-range hopping. Limits on the value of p are established and are used to show that only one existing theory of variable-range hopping is consistent with such a temperature dependence.

2. Experimental methods

Thin films of non-stoichiometric aluminium nitride of composition AlN_x were fabricated using voltage-controlled planar magnetron sputtering [32]. The deposition technique allows the deposition of films over a wide range of compositions by regulating the relative arrival rates of aluminium and nitrogen atoms at a substrate. Chromium/gold electrodes

were evaporated on Corning 7059 glass substrates which had previously been washed in trichlorethylene and isopropanol [33]. Following this first deposition, non-stoichiometric films of aluminium nitride of a thickness of ≈500 nm were deposited. It was decided to have the contact electrodes under the films instead of on their surfaces because of the rapidity with which the surface of non-stoichiometric films of aluminium nitride oxidises. At room temperature and pressure, a layer of ≈10 nm of Al_2O_3 forms within a period of 24 hours [34]. Following the deposition of the films, gold wires were cold welded to the electrodes using small amount of indium.

The conductivity of the films was measured between 10 K and room temperature using standard low-temperature techniques. The measurements were performed in a four-points probe configuration using an electrometer as a current source. Currents between 10^{-8} and 10^{-4} A were used depending upon the resistivity of the samples being measured. In all cases, the linearity of the resistance with the current was verified.

The Hall measurements were performed at room temperature in a magnetic field of 10^3 G. The experimental arrangement used is shown schematically in figure 1(*a*). In the absence of a magnetic field, an AC current of 10^{-4} A RMS at a frequency of 290 Hz was sent through the sample via the electrodes A and B (figure 1(*a*)). The differential voltage appearing between the points C and D was applied to a potentiometer. The voltage at the output of the potentiometer was then adjusted to null the voltage at point E. Turning on the magnetic field, a Hall voltage appears betwen point E and the output of the potentiometer. The advantage of this technique relies on the independence of the measured Hall voltage on the position of the contact electrodes.

The thermoelectric power was measured between 10 K and room temperature. The experimental arrangement used is shown in figure 1(*b*). One extremity of the glass substrate onto which a sample had been deposited was secured to a cold finger using vacuum grease. The average temperature of the sample was taken as that measured at

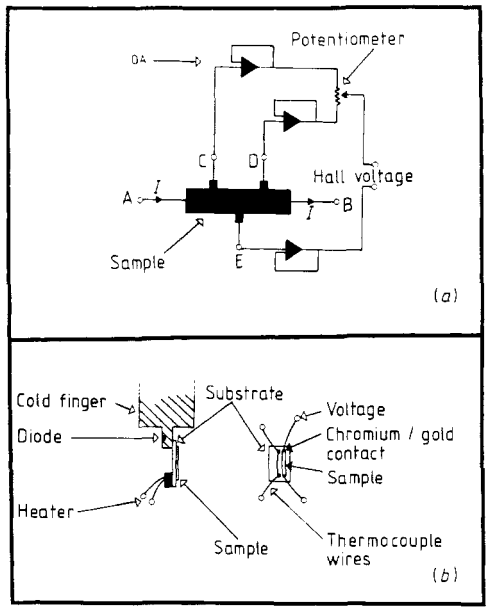

Figure 1. (*a*) Schematic of the experimental arrangement used in the measurement of the Hall effect (OA = operational amplifier). (*b*) Schematic of the experimental arrangement used in the measurement of the thermoelectric power.

the cold finger. This temperature was measured using a semiconducting diode. At the other extremity of the glass substrate was suspended a small resistive heater with which a temperature gradient could be applied along the length of the sample. Temperature gradients between 1 and 5 K were used. They were measured using thermocouple wires (chromel/alumel/chromel) mounted in a differential configuration. The thermocouple wires were cold welded with a very small amount of indium onto two evaporated chromium/gold electrodes located 0.5 mm away from both extremities of the sample. The measurements of the thermoelectric power were repeated at various values of ΔT and proved to be independent of the value of the temperature gradient. The thermoelectric power was calculated from the Seebeck relation $S = -\Delta V/\Delta T$. Two gold wires attached to the extremities of the sample were used to measure the voltage ΔV appearing across the sample. The same gold wires were used in all the measurements. Their contribution to the thermoelectric power was evaluated by first measuring the thermoelectric power of a gold/lead/gold thermocouple. Using the results of Roberts [35] for the thermoelectric power of lead, the contribution of the gold wires was deduced.

3. Film structure

Figure 2 shows the x-ray diffraction spectrum of non-stoichiometric films of aluminium nitride obtained using the 0.154 nm Cu–Kα radiation. The value of the room temperature conductivity of each film is also given on the figure.

The x-ray spectra of films with room temperature conductivity above 1200 Ω^{-1} cm^{-1} exhibit sharp aluminium lines. Broader and weaker aluminium nitride lines are also observed. These results suggest that films with a room-temperature conductivity above 1200 Ω^{-1} cm^{-1} are composed of very small particles of aluminium nitride dispersed in an aluminium matrix. This interpretation is supported by electron diffraction measurements and electron transmission photographs. Figure 3 shows a transmission photograph of a sample having a room temperature conductivity equal to 1500 Ω^{-1} cm^{-1}. This photograph reveals the existence of a columnar microstructure which is characteristic of vacuum-deposited coatings at low substrate temperature. The average column diameter observed in this photograph is $\approx$200 nm and corresponds to the size of the aluminium crystallites. The size of the aluminium nitride inclusions was estimated to be $\approx$10 nm from the line broadening observed in the x-ray spectrum. This value was obtained from the Sherrer relation [36] $t = 0.9\lambda/W \cos\theta_b$ where t is the particle size, λ the radiation wavelength, W the width of the spectral line, and θ_b the Bragg angle. This number should only be seen as an upper estimate since the influence of non-uniform strain on the line broadening is neglected in this analysis. The discontinuous appearance of the aluminium diffraction ring pattern observed in an electron diffraction photograph of a film having a room temperature conductivity of 10^4 Ω^{-1} cm^{-1} (figure 4(*a*)) indicates that the aluminium crystallites grow with a strongly preferred orientation of the *c*-axis perpendicular to the substrate. Broader and continuous aluminium nitride rings are also clearly observed, which indicate that the aluminium nitride grains are very small ($\leqslant$10 nm) and grow with a random orientation.

Returning to figure 2, it is observed that the reduction of the film conductivity from 1200 to 700 Ω^{-1} cm^{-1} is accompanied by a reduction of the aluminium lines intensities and an increase of their linewidths, indicating a tendency of the aluminium crystallites to break up into smaller units. The intensities of the aluminium nitride lines increase slightly while their linewidths remain broad, suggesting that the number of aluminium

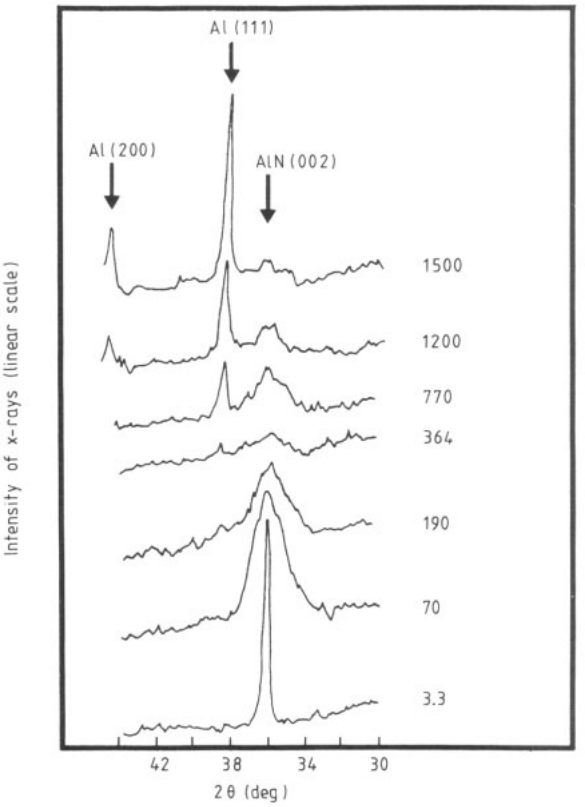

Figure 2. X-ray diffraction spectrum of non-stoichiometric films of aluminium nitride. The room temperature conductivity of each film is given in the figure in $\Omega^{-1}\,cm^{-1}$.

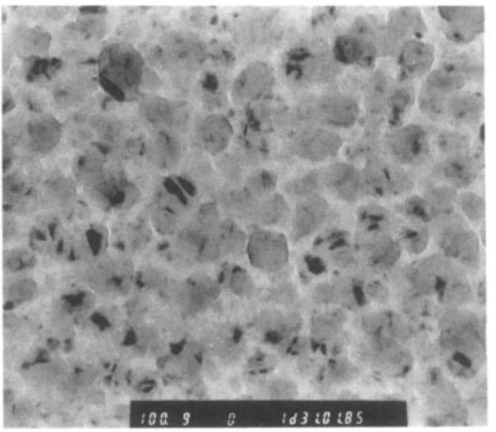

Figure 3. Electron transmission photograph showing the columnar microstructure characteristic of vacuum deposited coatings at low substrate temperature. The room temperature conductivity of this film is $1.5 \times 10^4\,\Omega^{-1}\,cm^{-1}$.

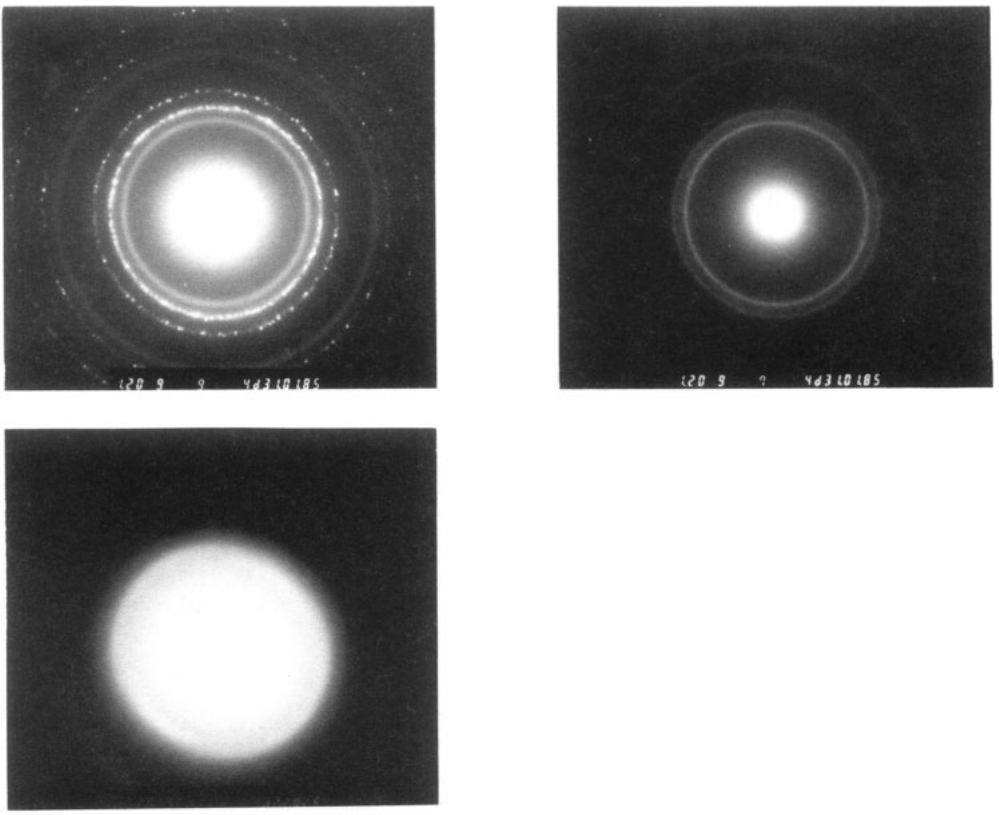

Figure 4. Electron diffraction measurements: (*a*) of a film with room temperature conductivity of $10^4\ \Omega^{-1}\ cm^{-1}$; (*b*) of a film with room temperature conductivity of $600\ \Omega^{-1}\ cm^{-1}$; (*c*) of a film with room temperature conductivity of $200\ \Omega^{-1}\ cm^{-1}$.

nitride particles is increasing while their sizes remain quite small ($\leqslant 10$ nm). The aluminium rings observed in an electron diffraction photograph of a film having a room temperature conductivity of $600\ \Omega^{-1}\ cm^{-1}$ have a continuous appearance (figure 4(*b*)) as opposed to the spotty ring structure observed in films of higher conductivity (figure 4(*a*)). This indicates that the aluminium crystallites lose their preferred growing orientation as the film conductivity decreases. Films with room-temperature conductivity between 400 and $200\ \Omega^{-1}\ cm^{-1}$ can be best described as being amorphous. Their x-ray spectra only reveal broad lines of low intensities (figure 2). These films appear completely structureless in the electron transmission photographs. In electron diffraction measurements the films only yield broad, diffuse rings (figure 4(*c*)). From the above observations it can be concluded that the reduction of the film conductivity from $1.5 \times 10^4\ \Omega^{-1}\ cm^{-1}$ to $200\ \Omega^{-1}\ cm^{-1}$ is accompanied by an increase in the structural disorder present in these films.

As the film conductivity is reduced below $200\ \Omega^{-1}\ cm^{-1}$ the aluminium nitride lines of the x-ray spectrum gain in strength and their linewidths decrease, indicating an increase in the volume fraction and size of the aluminium nitride particles. The aluminium x-ray lines remain very weak and are not observed in films with room temperature conductivity below $10\ \Omega^{-1}\ cm^{-1}$. Nevertheless, the high value of the room temperature

conductivity of these films clearly suggest that they contain aluminium atoms in excess. It is concluded that the aluminium atoms are either finely dispersed in an aluminium nitride matrix (acting as dopant) or that they form small metallic islands with an amorphous structure. Similar results have been observed in non-stoichiometric films of zinc oxide: while these films were known to contain zinc atoms in excess, no zinc lines were observed in the x-ray spectrum of the films [37].

4. Transport properties

4.1. Regime of moderate disorder: DC conductivity

Samples with a room temperature conductivity about $10^4\ \Omega^{-1}\ cm^{-1}$ exhibit a metallic behaviour well described by the Boltzmann equation $\sigma = (ne^2/mv_f)l$, where n is the number of charge carriers per cm^3, e the electronic charge, m the electronic mass, v_f the Fermi velocity, and l the electronic mean free path.

The temperature dependence of the conductivity of samples with a room temperature conductivity between 10^3 and $10^4\ \Omega^{-1}\ cm^{-1}$ is characterised by a broad maximum at a temperature T_m (figures 5–8). With increasing temperature the conductivity first increases as $T^{1/2}$ until the maximum in conductivity is reached (figures 5 and 6). Above that temperature the conductivity decreases linearly with T (figures 7 and 8). Also it is observed that the value of T_m for a given sample is a function of the magnitude of the conductivity (figures 7 and 8). Samples with low room temperature conductivity have high values of T_m while samples with high room temperature conductivity have low values of T_m. Samples with room temperature conductivity between 10^3 and $100\ \Omega^{-1}\ cm^{-1}$ do not exhibit a conductivity maximum in the temperature range examined. Instead, the conductivity increases continuously as $T^{1/2}$ as the temperature is increased between 10 and 300 K (figure 9). Presumably, the conductivity maximum has been shifted to temperatures well above 300 K. Finally, the $T^{1/2}$ behaviour is no longer observed in samples with a room temperature conductivity less than $100\ \Omega^{-1}\ cm^{-1}$ (figure 10).

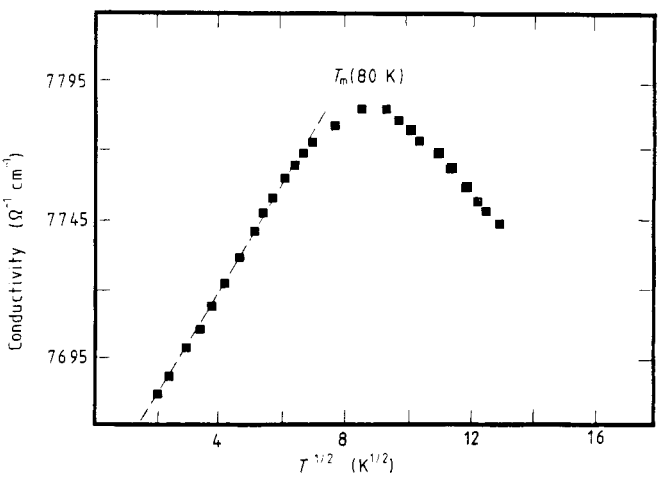

Figure 5. Temperature dependence of the DC conductivity of a film having a room temperature conductivity equal to $7740\ \Omega^{-1}\ cm^{-1}$. A $T^{1/2}$ behaviour is observed below the conductivity maximum at 80 K.

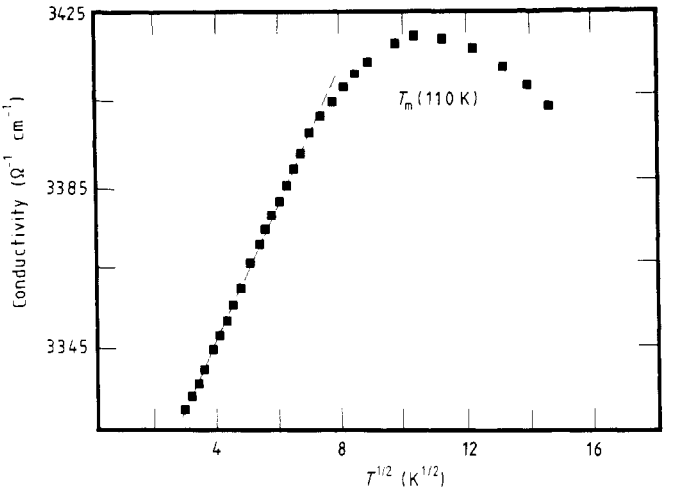

Figure 6. Temperature dependence of the DC conductivity of a film having a room temperature conductivity equal to 3400 Ω^{-1} cm^{-1}. A $T^{1/2}$ behaviour is observed below the conductivity maximum at 110 K. One notes that the conductivity maximum occurs at a higher temperature than for the sample of figure 5.

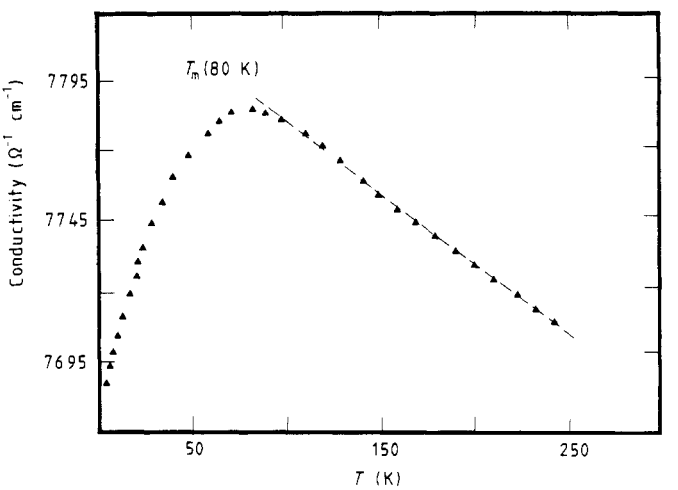

Figure 7. Temperature dependence of the DC conductivity of a film having a room temperature conductivity equal to 7740 Ω^{-1} cm^{-1}. A linear behaviour is observed above the conductivity maximum (80 K).

These experimental observations are found to be accurately described by equation (2) of Kaveh and Mott [2, 21] if it is assumed that the main scattering mechanism of electrons are phonons and that the inelastic mean free path l_i has the high-temperature form $l_i \propto T^{-1}$. With $l_i = aT^{-1}$, (2) can be written as:

$$\sigma = \sigma_b(0)\left\{1 - \frac{3}{(k_f l_e)^2}\right\} + \sigma_b(0)\left\{\frac{3^{3/2}}{(k_f l_e)^2}(l_e/a)^{1/2}T^{1/2} - (l_e/a)T\right\}. \qquad (3)$$

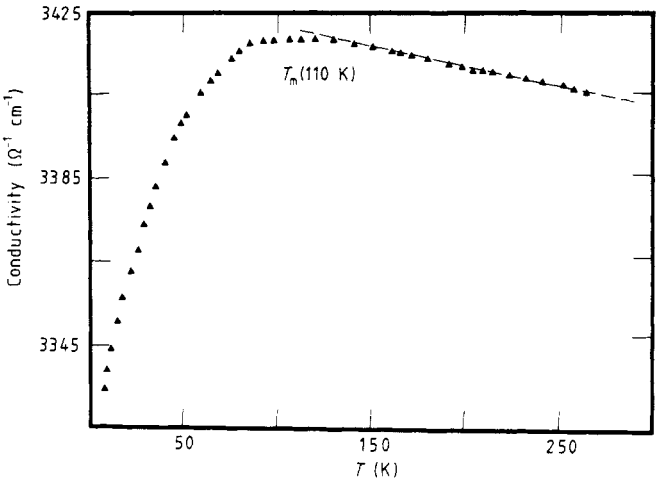

Figure 8. Temperature dependence of the DC conductivity of a film having a room temperature conductivity equal to 3400 Ω^{-1} cm^{-1}. A linear behaviour is observed above the conductivity maximum (110 K).

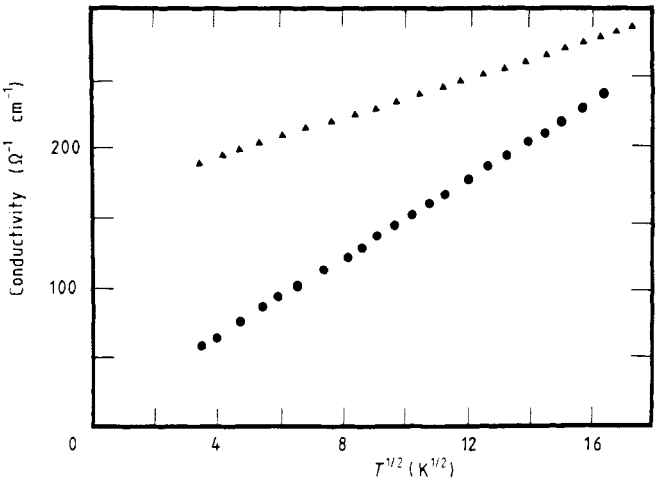

Figure 9. Temperature dependence of the DC conductivity of two films showing a $T^{1/2}$ behaviour between 10 K and room temperature.

One notes that this equation has a maximum at T_m given by:

$$T_m = (27/4)\left\{\frac{a}{K_f^4 l_e^5}\right\}. \tag{4}$$

The results of § 3 indicate that the reduction of the room temperature conductivity of the deposited films from 1500 to 200 Ω^{-1} cm^{-1} is accompanied by an increase in structural disorder. This should in turn lead to a smaller elastic mean free path l_e. The form of T_m is therefore consistent with the experimental observation that the small the room temperature conductivity of a film, the higher its value of T_m (figures 7 and 8). Moreover, (3) predicts that for temperatures well above T_m, the temperature dependence of the

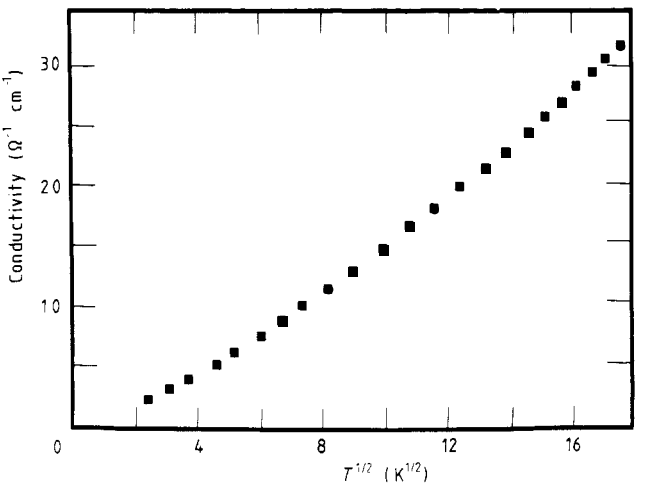

Figure 10. Temperature dependence of the DC conductivity of a film with a room temperature conductivity smaller than 100 Ω^{-1} cm^{-1}. A deviation from the $T^{1/2}$ behaviour is observed.

conductivity of a given film should be dominated by the term linear in T while for temperatures well below T_m it should be dominated by the term in $T^{1/2}$, a temperature dependence which is observed experimentally (figures 5–8). Finally, for large enough disorder and small values of the elastic mean free path l_e, the $T^{1/2}$ term of (3) should completely dominate the temperature dependence of the conductivity and no conductivity maximum should be observed in the temperature range examined. Such a temperature dependence is observed in figure 9. All the temperature dependences predicted by (3) are therefore observed experimentally. From figures 5–9 and equation (3), the values of l_e and l_i for each sample have been evaluated and the results are summarised in table 1. The values of K_f were estimated using the free-electron formula $k_f = (3\pi^2 n)^{1/3}$ and the values of n determined from Hall measurements. This analysis shows that the values of a, l_e and K_f needed to recover the correct magnitude for the conductivity are physically reasonable. Moreover, the derivation of (3) is valid only for $(K_f l_e)^2 \gg 3$. It is found that all samples with room-temperature conductivity $\geqslant 100\ \Omega^{-1}$ cm^{-1} for which (3) provides an accurate description of their temperature dependence yield values of $(K_f l_e)^2 \gg 3$. On the other hand, samples with room-temperature conductivity $\leqslant 100\ \Omega^{-1}$ cm^{-1} are found to be poorly described by (3) and yield

Table 1.

σ(300 K) (Ω^{-1} cm^{-1})	$\sigma(0)$ (Ω^{-1} cm^{-1})	K_f (cm^{-1})	l_e (cm)	$(K_f l_e)^2$ (–)	a (cm T^{-1})
3.1×10^4	4.3×10^4	1.38×10^8	2.7×10^{-7}	1.4×10^3	1.8×10^{-4}
1.9×10^4	2.41×10^4	1.30×10^8	1.7×10^{-7}	4.8×10^2	1.4×10^{-4}
4.1×10^3	3.4×10^3	1.0×10^8	4.3×10^{-8}	18.5	2.6×10^{-5}
1.3×10^3	1.1×10^3	8.8×10^7	3.0×10^{-8}	7	3.2×10^{-4}
1.1×10^3	9.9×10^2	8.7×10^7	2.9×10^{-8}	6.5	4.3×10^{-4}
2.9×10^2	1.5×10^2	6.6×10^7	2.8×10^{-8}	3.5	1.4×10^{-3}
2.3×10^2	10	6.2×10^7	2.8×10^{-8}	3.0	3.4×10^{-4}

values of $(K_f l_e)^2 \approx 3$, thus at the limit of validity of (3). One should not expect (3) to provide an accurate description of the temperature dependence of these samples. It is concluded that the conductivity of the films produced in this work, with a room temperature conductivity between 10^4 and 100 Ω^{-1} cm^{-1} is dominated by localisation effects and that equation (3) of Kaveh and Mott [2, 21] provides a good description of both the magnitude and the temperature dependence of the conductivity.

4.2. Regime of moderate disorder: thermoelectric power and Hall effect

The correction to the Boltzmann conductivity (equations (1) and (3)) was obtained by Kaveh and Mott [19] by using power-law localised wavefunctions of the form $\Psi_E \propto e^{ik\cdot r}/r^2$ and calculating the conductivity using the Kubo–Greenwood formalism [38]. In order to recover the scaling result of Abrahams *et al* [31] they also assumed that the density of states remains free-electron like, that is $N(E)$ is unaffected by localisation effects.

The correctness of this assumption might be verified by measuring the thermoelectric power. The correction to the Boltzmann conductivity given by (1) and (3) is energy independent. As localisation effects set in, $\sigma(E)$ and σ are modified according to (1) and (3). Nevertheless the contribution of the conduction at a given energy $\sigma(E)$ relative to the total conduction σ remains unchanged. This suggests that no correction to the thermoelectric power is expected, since $S(T)$ can be written as [39]:

$$S = -\frac{k}{e}\int \left(\frac{(E - E_f)}{kT}\right)\frac{\sigma(E)}{\sigma}\,dE. \tag{5}$$

Figure 11 shows the temperature dependence of the thermoelectric power of samples for which the conductivity is characterised by a $T^{1/2}$ behaviour between 10 and 300 K. Above $\approx$100 K, the thermoelectric power increases linearly with T, as expected for a metal. These results suggest that the dependence of S on T is free-electron like and support the assumption that the density of states remains free-electron like as localisation effects set in.

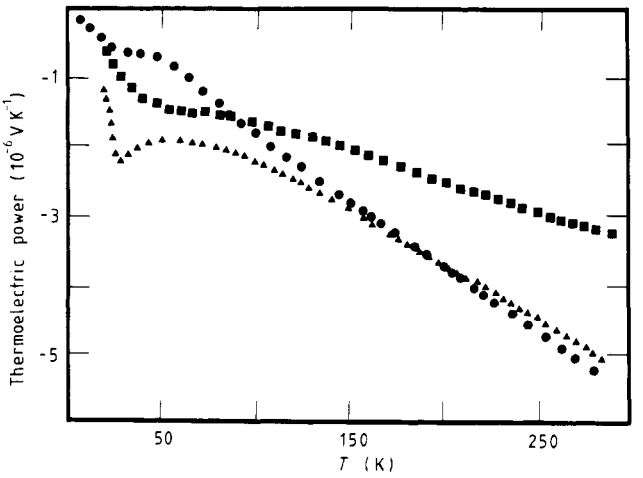

Figure 11. Temperature dependence of the thermoelectric power of three films for which the DC conductivity exhibits a $T^{1/2}$ behaviour between 10 K and room temperature.

Assuming that the free-electron expression

$$S(T) = -\frac{4\pi^4}{3e}\frac{m}{h^2(3\pi^2)^{2/3}}\frac{T}{n^{2/3}} \tag{6}$$

(where k and h are the Boltzmann and Planck constants respectively) holds, the values of n can be extracted from the slopes of $S(T)$. These values of n are plotted as a function of the room-temperature conductivity in figure 12.

The verification of the dependence of the thermoelectric power on n requires an independent measurement of n. This can be done using the Hall effect. Because of the assumption that the density of states is unaffected by localisation effects, the free-electron expression,

$$n = \frac{H}{ect}\left(\frac{I}{V_{\text{hall}}}\right) \tag{7}$$

(where I is the current, H the magnetic field, V_{Hall} the measured Hall voltage, t the thickness of the sample, and c the speed of light) is valid. This can simply be shown. Since the density of states is assumed to remain free-electron like, it follows that n does not change, the two quantities being related to one another by the expression, $N(E) = \frac{3}{2}(n/E_f)(E/E_f)^{1/2}$. The correction to the conductivity can therefore be expressed in terms of a varying lifetime, gradually varying from its free-electron value τ to a new value τ^*. The resulting conductivity can be written as:

$$\sigma = \sigma_b\left\{1 - \frac{3}{(k_f l_e)^2}\left(1 - \frac{l_e}{L_i}\right)\right\}$$

$$\sigma = \frac{ne^2\tau^*}{m} \tag{8}$$

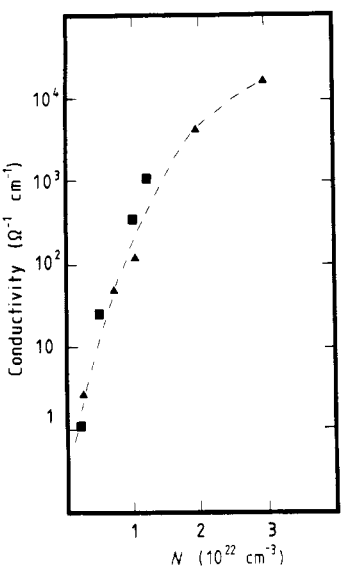

Figure 12. Charge carriers density (n) plotted as a function of the room temperature conductivity. Triangles: as determined from thermoelectric power measurements. Squares: as determined from Hall measurements.

In the evaluation of the Hall voltage we are led to consider an equation of the form [40]:

$$\sigma E_y = -\left(\frac{eH}{mc}\right)\tau^* J_x + J_y \tag{9}$$

where J_x is the current density in the x-direction, and E_y and J_y are the transverse electric field and the current density in the y-direction respectively. The Hall field is determined by the requirement that there is no transverse current J_y. Setting $J_y = 0$ in (9) leads to:

$$\frac{E_y}{J_x} = \left(\frac{eH}{mc}\right)\frac{\tau^*}{\sigma}. \tag{10}$$

Since $\sigma = (ne^2\tau^*/m)$, the τ^* cancel out and all the effects related to electron localisation disappear from (10). With $J_x = I/(\omega t)$ and $V_{\text{Hall}} = -E_y W$, where W is the width of the sample, the free-electron formula (7) can be recovered from (10).

On figure 12, the values of n obtained from Hall measurements are plotted as a function of the room temperature conductivity. Within the experimental errors, the same values of n are obtained from the thermoelectric power measurements and the Hall effects measurements. These results therefore suggest that the dependence of the thermoelectric power and the Hall effect on n is free-electron like. These results are seen as strongly suggesting that the density of states is indeed unaffected by localisation effects.

These experimental results are in agreement with those obtained by Thomas [41] upon comparing the dependence of the conductivity and electronic specific heat on the density of charge carriers n. Thomas found that while the dependence of the conductivity σ on n was dominated by localisation effects, the dependence of the electronic specific heat on n remained free-electron like, supporting the idea that the density of states is essentially unaffected by localisation effects.

The low-temperature behaviour of the thermoelectric power is tentatively attributed to phonon drag. This effect usually dominates the temperature dependence of the thermoelectric power of metals at low temperature. A crude estimate of the phonon drag contribution to the thermoelectric power is given by [42] $S_g \approx C_v/ne$ where C_v is the lattice specific heat. The total thermoelectric power S, including the electronic (S_e) and phonon contributions S_g, can then be approximated by [42]

$$S = C_v/ne + C_e/ne \tag{11}$$

whre C_e is the electronic specific heat. At low temperatures, $C_e \approx T$ and $C_v \approx T^3$ and (11) is often written as $S/T = aT^2 + b$. If phonon drag dominates the thermoelectric power at low temperatures, S/T varies as T^2 and the extrapolated value of S/T at $T =$ 0 K yields the slope of the electronic component of the thermoelectric power (S_e/T). The results of S/T plotted as a function of T^2 are shown in figure 13. While the accuracy of the data is not sufficient to convincingly show that S/T is indeed proportional to T^2, the extrapolated value of S/T at $T = 0$ K approximately yields the correct values for S_e/T.

4.3. Regime of strong disorder

As discussed in the introduction, the limit of very strong disorder the wavefunctions are expected to become exponentially localised and the conductivity to proceed via either nearest-neighbour hopping and/or variable-range hopping. In term of their resistivity,

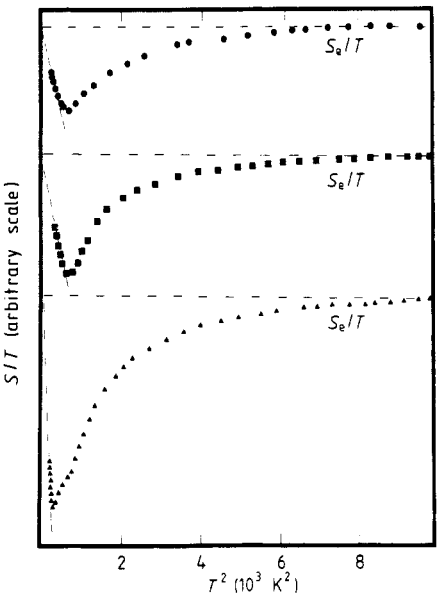

Figure 13. S/T plotted as a function of T^2. The extrapolation of S/T to $T = 0$ K approximately yields the slope of the electronic contribution to the thermoelectric power (S_e/T), indicating that the low-temperature behaviour of the thermoelectric power might be attributed to phonon drag.

ρ, both conduction mechanisms are characterised by a temperature dependence of the form

$$\rho(T) = \rho_0 T^p \exp(T_0/T)^s \tag{12}$$

with $s = 1$ for nearest-neighbour hopping and $s = \frac{1}{4}$ for variable-range hopping [43]. For the latter, $s = \frac{1}{2}$ is expected if Coulomb interactions are strong enough to open a gap in the density of states at the Fermi level [44]. The value of the exponent p depends on the form of the wavefunctions and the method used to calculate the conductivity. This temperature dependence is weak and usually masked by the exponential term $\exp(T_0/T)^s$. Very few attempts have therefore been made to determine experimentally the value of p. Nevertheless, this weak-temperature dependence may provide a criterion for determining experimentally which of the existing theories of variable-range hopping gives the best description to the temperature dependence of the conductivity.

The present theories of variable-range hopping (Allen *et al* [45], Mott [46], Pollack [47] and Shklovskii [48]) are based on the expression for the electron transition probability between two sites i and j, first calculated by Miller and Abrahams [49]. For hydrogenic wavefunctions it takes the form [50]:

$$\gamma_{ij} = \frac{16\pi^3 E_1^2 \varepsilon_{ij}}{\mathrm{d}s^5 h^4} \left(\frac{2e^2\alpha}{3\kappa}\right)^2 (\alpha r_{ij})^2 \left[1 + \left(\frac{\pi\varepsilon_{ij}}{h\alpha s}\right)^2\right]^{-4} \eta(\varepsilon_{ij}) \exp(-2\alpha r_{ij}) \tag{13}$$

where E_1 is the deformation potential, ε_{ij} is the hopping energy, d the density, s the speed of sound, κ the dielectric constant, α the decay rate of the wavefunction, r_{ij} the intersite distance and $\eta(\varepsilon_{ij})$ the number of phonons with energy ε_{ij}. It is assumed that the term $\pi\varepsilon_{ij}/h\alpha s$ is small and thus neglected. Variable-range hopping theories differ from

one another by the method used to calculate the macroscopic conductivity. Allen *et al* [45], using diffusion equations, obtain the following expression for the macroscopic conductivity, $\sigma \propto e^2\gamma_{ij}/(R_{max}kT)$, where $R_{max} = (1/2\alpha)(T_0/T)^{1/4}$ is the typical hopping distance between two sites i and j at a temperature T. Upon substituting γ_{ij} (13) in their expression for σ they obtain:

$$\rho = \rho_0 T^{1/2} \exp(T_0/T)^{1/4} \tag{14}$$

Shklovskii [48] and Pollack [47] use a different length scale in their expression for the conductivity given by $\sigma \propto (1/L_0)(e^2\gamma_{ij}/kT)$, where $L_0 = (1/2\alpha)(T_0/T)^{1/2}$. This different length scale (L_0 instead of R_{max}) leads to another temperature dependence for the conductivity given by:

$$\rho = \rho_0 T^{1/4} \exp(T_0/T)^{1/4}. \tag{15}$$

Finally, Mott [46] starting with $\sigma = e^2N(\varepsilon)R_{max}^2\gamma_{ij}$ obtains:

$$\rho = \rho_0 T^{-1/4} \exp(T_0/T)^{1/4}. \tag{16}$$

It was observed that the temperature dependence of samples with room temperature conductivity $\leqslant 0.5\ \Omega^{-1}\,cm^{-1}$ was very strong and attempts were made at fitting the experimental data between 10 K and room temperature to an equation of the general form (12). As a first approximation, the exponent p was set to zero and the correlation coefficient R [51] was calculated for various values of s. A value of $R = 1$ corresponds to a perfect fit, while a value of $R = 0$ indicates that the data cannot be fitted by a function of the form (12). Typical results are shown in figure 14 and indicate that a value of $s = 0.25$ provides the best fit to the experimental data. Other attempts were made at fitting independently high- and low-temperature regions. None of these attempts were successful. Using a value of $s = 0.25$, limits on the value of p were then established. It was found that the best fits were obtained with values of p between $0.3 \leqslant p \leqslant 0.9$. Deviations were clearly observed when using values of p outside this interval (figure 15). In figure 16 is shown the temperature dependence of two samples obtained using

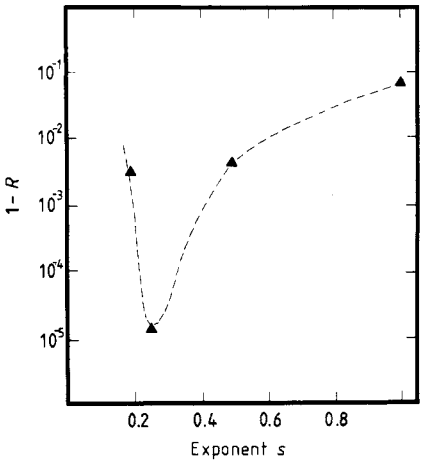

Figure 14. $(1 - R)$, where R is the correlation coefficient, plotted as a function of the exponent s, showing that the value $s = 0.25$ provides the best fit to the experimental data of the conductivity between 10 K and room temperature.

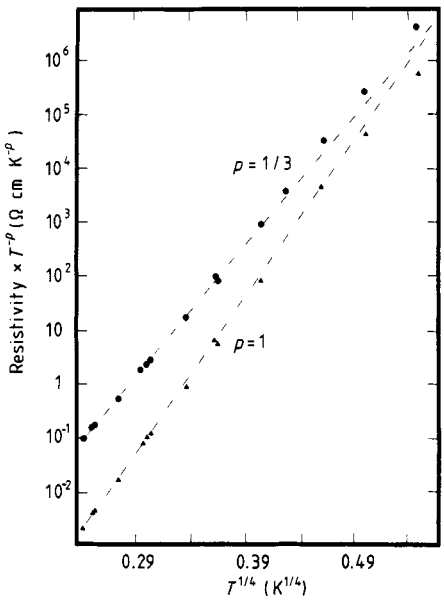

Figure 15. Temperature dependence of the DC conductivity of a film with room temperature conductivity of 0.5 Ω^{-1} cm^{-1} plotted using the two limits established on the value of p. Deviation from the temperature dependence predicted by (12) is observed when using values of $p \leqslant \frac{1}{3}$ and $p \geqslant 0.9$.

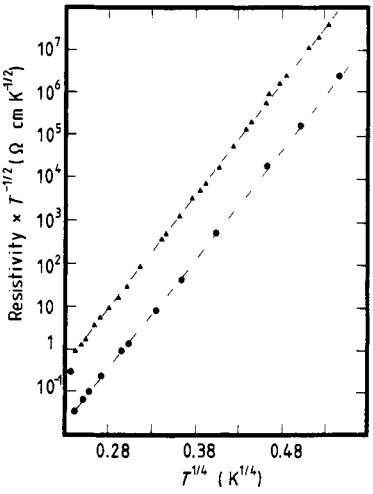

Figure 16. Temperature dependence of the DC conductivity of two samples using $p = 0.5$ and $s = 0.25$. No deviation from the temperature dependence predicted by (12) are observed between 10 K and room temperature.

$p = 0.5$ and $s = 0.25$. For these values of s and p, no deviations from the temperature dependence predicted by (12) are observed between 10 K and room temperature.

Only the theory of Allen [45] (14), with a value of $p = 0.5$, is consistent with the limits established experimentally on the value of p. The theories of Shklovskii [48] ($p = 0.25$), Pollack [47] ($p = 0.25$) and Mott [46] ($p = -0.25$) predict values of p which are not

observed experimentally in our samples. These results indicate that the expression for the conductivity $\sigma \propto e^2\gamma_{ij}/(R_{max}kT)$, with the length scale chosen as R_{max} instead of L_0, leads to the best description to the temperature dependence of the conductivity observed in these samples.

Estimates of α and $N(\varepsilon_f)$, the density of states at the Fermi level, have been obtained for various samples from the experimental values of ρ_0 and T_0, by solving the equations,

$$\rho_0 = \frac{36\pi^3 m^2}{(2\pi)^{1/2}} \left(\frac{ds^5}{e^2 E_1^2}\right)\left(\frac{kN(\varepsilon_f)}{\alpha^{13}}\right)^{1/2} \tag{17}$$

(where $\varepsilon\varepsilon_0$ has been replaced by $\varepsilon\varepsilon_0 = \pi me^2/h^2\alpha$) [52] and

$$T = \frac{18N(\varepsilon_f)}{k\alpha}. \tag{18}$$

These expressions have been obtained from the model of Allen *et al* [45]. The parameters d, s and E_1 were assumed to be constant for all the samples and the values $d = 10^3$ kg m^{-3}, $s = 4 \times 10^3$ m s^{-1} and $E_1 = 1.6 \times 10^{-18}$ J were used. It was verified that in all cases the condition $\pi\varepsilon_{ij}/hs\alpha \ll 1$ (where $\varepsilon_{ij} \approx kT(T_0/T)^{1/4}$) was met. The results of this analysis are summarised in table 2. They indicate that the theory of Allen [45] predicts values of α and $N(\varepsilon_f)$ that are physically acceptable. One notes nevertheless that the condition $\varepsilon_{ij}/2hs\alpha \ll 1$ is barely met.

Table 2.

ρ(300 K) (Ω^{-1} cm^{-1})	ρ_0 (Ω cm/$K^{1/2}$)	T_0	α (cm^{-1})	$N(\varepsilon_f)$ (eV^{-1} cm^{-3})	$\varepsilon_{ij}/2hs\alpha$ (—)
31	5.6×10^{-10}	7.2×10^7	3.8×10^7	1.6×10^{20}	0.3
9	1.8×10^{-7}	1.1×10^7	1.2×10^7	3.2×10^{19}	0.7
0.34	3.2×10^{-8}	9.3×10^6	1.6×10^7	1×10^{20}	0.5

5. Conclusions

Films of non-stoichiometric aluminium nitride of composition AlN_x were fabricated using DC reactive sputtering. The room-temperature conductivity of the deposited films was varied between $5 \times 10^4\ \Omega^{-1}$ cm^{-1} and $10^{-3}\ \Omega^{-1}$ cm^{-1} by regulating the relative arrival rates of nitrogen and aluminium atoms on a substrate. The structure and transport properties of these films were examined. It was found that the structure of films with a room temperature conductivity above $10^4\ \Omega^{-1}$ cm^{-1} is characterised by small aluminium nitride particles ($\approx$ 10 nm in diameter) dispersed in a polycrystalline aluminium matrix. The size of the aluminium crystallites is about 200 nm. The temperature dependence of the conductivity of these films is well described by the Boltzmann transport equations, thus indicating that the electron wavefunctions are extended.

Increasing the number of nitrogen atoms impinging the substrate relative to that of the aluminium atoms leads to a break-up of the aluminium crystallites into smaller units and to a larger number of small aluminium nitride particles. This process continues until the deposited films become amorphous. This increase in structural disorder is accompanied by a decreasing room temperature conductivity from 10^4 to 400 Ω^{-1} cm^{-1},

the conductivity at which the structure of these films become amorphous. The temperature dependence of films with such room temperature conductivities is accurately described by the diffusion model of Kaveh and Mott (2). It indicates that localisation effects dominate the DC conductivity and that the envelopes of the electron wavefunctions are decaying as a power law. Above 100 K, the dependence of the thermoelectric power of these films on n and T is found to be free-electron like. These results are interpreted as indicating that the density of states $N(E)$ essentially retains its free-electron form even as localisation effects set in.

The temperature dependence of films with room temperature conductivity between 0.5 and $10^{-3}\,\Omega^{-1}\,\mathrm{cm}^{-1}$ is well described by (12) with $s = 0.25$ and p between $0.3 \leqslant p \leqslant 0.9$. This temperature dependence is consistent with the variable-range hopping model proposed by Allen [45]. It is found that this theory also predicts values of α and $N(\varepsilon_f)$ that are physicaly acceptable. The variable-range hopping model of Mott [46], Pollack [47] and Shklovskii [48] yield values of the exponent p which are not observed experimentally in our samples.

Acknowledgments

We would like to thank Dr R Barrie and Mark Shegelski for many useful discussions of this work.

References

[1] Howson H A and Greig D 1984 *Phys. Rev.* B **30** 4805
[2] Howson H A 1984 *J. Phys. F: Met. Phys.* **14** L25
[3] Saub K, Babic E and Ristic R 1985 *Solid State Commun.* **53** 269
[4] Van der Dries L, Van Haesendonock C and Bruynseraede Y 1981 *Phys. Rev. Lett.* **46** 565
[5] Rosembaum T F, Andres K, Thomas G A and Lee P A 1981 *Phys. Rev. Lett.* **46** 568
[6] Cochrane R W, Harris R, Strom-Olson J O and Zuckermann M J 1975 *Phys. Rev. Lett.* **35** 676
[7] McAlister S P, Inglis A D and Kroeker D R 1984 *J. Phys. C: Solid State Phys.* **17** L751
[8] Vergnat M, Marchal G, Piecuch M and Gerl M 1984 *Solid State Commun.* **50** 237
[9] Scharein R G and Williams G 1984 *Phys. Rev.* B **30** 3506
[10] de Kort K 1984 *J. Phys. C: Solid State Phys.* **17** 5237
[11] Abraham D and Rosembaum R 1984 *J. Phys. C: Solid State Phys.* **17** 2627
[12] Cochrane R W and Strom-Olsen J O 1984 *J. Phys. B: At. Mol. Phys.* **29** 1088
[13] Giordano N 1980 *Phys. Rev.* B **22** 5635
[14] Giordano N, Gilson W and Kroeker D R 1979 *Phys. Rev. Lett.* **43** 725
[15] Dolan G J and Osheroff D D 1979 *Phys. Rev. Lett.* **43** 721
[16] Kaveh M and Mott N F 1981 *J. Phys. C: Solid State Phys.* **14** L183
[17] Kaveh M and Mott N F 1981 *J. Phys. C: Solid State Phys.* **14** L177
[18] Kaveh M and Mott N F 1982 *J. Phys. C: Solid State Phys.* **15** L697
[19] Kaveh M and Mott N F 1983 *J. Phys. C: Solid State Phys.* **16** L1067
[20] Kubo R 1952 *Phys. Rev.* **86** 929
[21] Kaveh M and Mott N F 1982 *J. Phys. C: Solid State Phys.* **15** L707
[22] Beck H and Nettle S 1984 *Phys. Lett.* **105A** 319
[23] Inglis A D and McAlister S P 1985 *Solid State Commun.* **54** 331
[24] Gogolin A A and Zimanyi T 1983 *Solid State Commun.* **46** 469
[25] Lee P A and Ramakrishnan T V 1985 *Rev. Mod. Phys.* **57** 287
[26] Gogolin A A and Zimanyi T 1976 *Sov. Phys.-JETP* **42** 168
[27] Thouless D J 1977 *Phys. Rev. Lett.* **39** 1167
[28] Anderson P W, Abrahams E and Ramakrishnan T V 1979 *Phys. Rev. Lett.* **43** 718
[29] Gogolin A A 1982 *Phys. Rep.* **86** 1

[30] Anderson P W 1958 *Phys. Rev.* **109** 1492
[31] Abrahams E, Anderson P W, Licciardello D C and Ramakrishnan T V 1979 *Phys. Rev. Lett.* **42** 673
[32] Affinito J and Parsons R R 1984 *J. Vac. Sci. Technol.* A **2(3)** 1275
[33] Brown R 1970 *Handbook of Thin Film Technology* (New York: McGraw-Hill) p 6–39
[34] Affinito J 1984 *PhD Thesis* University of British Columbia
[35] Roberts R B 1977 *Phil. Mag.* **36** 91
[36] Cullity B 1959 *Elements of X-Ray Diffraction* (London: Addison-Wesley) p 99
[37] Brett M 1985 *PhD Thesis* University of British Columbia
[38] Mott N F and Davis E A 1979 *Electronic Processes in Non-Crystalline Materials* (Oxford: OUP) 2nd edn
[39] Fritzsche H 1971 *Solid State Commun.* **9** 1813
[40] Ashcroft N W and Mermin N D 1976 *Solid State Phys.* (Philadelphia: Saunders) p 13
[41] Thomas G A, Ootaka Y and Kobayashi S 1981 *Phys. Rev.* B **24** 4886
[42] Huebener R D 1972 *Solid State Physics* **27** (New York: Academic) p 63
[43] Mott N F 1969 *Phil. Mag.* **19** 835
[44] Efros A L and Shklovskii B I 1975 *J. Phys. C: Solid State Phys.* **8** L49
[45] Allen F R and Adkins C J 1972 *Phil. Mag.* **26** 1027
[46] Mott N F 1972 *J. Non-Cryst. Solids* **8–10** 1
[47] Pollack M 1972 *J. Non-Cryst. Solids* **8–10** 486
[48] Shklovskii B I and Efros A L 1984 *Electronic Properties of Doped Semiconductors* (Berlin: Springer) ch 9
[49] Miller A and Abrahams E 1960 *Phys. Rev* **120** 745
[50] Shklovskii B I and Efros A L 1984 *Electronic Properties of Doped Semiconductors*, (Berlin: Springer) ch 4
[51] Bevington P R 1969 *Data Reduction and Error Analysis for the Physical Sciences* (New York: McGraw-Hill) ch 7 119
[52] Shklovskii B I and Efros A L 1984 *Electronic Properties of Doped Semiconductors* (Berlin: Springer) ch 1